

Comparison of patch-based and synoptic connectivity algorithms with graph theory metrics. A case study in Reggio Calabria metropolitan area (South Italy)

Giovanni Lumia^a, Giuseppe Modica^{b,*}, Salvatore Praticò^a, Samuel Cushman^c

^a Dipartimento di Agraria, Università Degli Studi 'Mediterranea' di Reggio Calabria, 89122 Reggio Calabria, Italy

^b Dipartimento di Scienze Veterinarie, Università Degli Studi di Messina, 98168 Messina, Italy

^c University of Oxford, Department of Biology, Wildlife Conservation Research Unit, 11a Mansfield Road, Oxford OX1 3SZ, United Kingdom

ARTICLE INFO

Keywords:

Landscape connectivity
Ecological network
Animal movement simulations
Dispersal thresholds
Source points distribution
Multivariate statistics

ABSTRACT

Context: Predicting and mapping connectivity between habitats and populations is critical to addressing habitat loss and biodiversity issues. Several strategies in the literature exist to understand, restore, and preserve ecological connectivity. The main issue of the current research is to identify which connectivity modeling strategies are the most reliable for planning purposes.

Objectives: Our goals in this paper were to compare connectivity predictions using a wide variety of commonly used approaches to improve the understanding of the similarities and differences in the predictions of these methods. Specifically, we investigated the differences in connectivity predictions related to the connectivity algorithm, the number and distribution of source points, and the threshold distance at which connectivity is allowed between locations. First, we separately applied different strategies and methods commonly used in the literature to model connectivity in the same study area. Then, going through a series of hypotheses, we compared the different models to confirm or disprove the initial hypotheses.

Methods: We proposed 4 main hypotheses and 14 combinations of them, hypothesizing that what most influences the results of connectivity models are different dispersal distance thresholds; differences in connectivity algorithms, especially kernel, path, and graph theory-based approaches; differences in predictions produced by two different software tools, UNICOR and Graphab; use of source points derived from a synoptic or patch-based perspective.

Results: We found that the dominant pattern of differences in the predictions of different connectivity analyses was related to the method of analysis, with clear differences between kernel, path, and graph-theory approaches and relatively little effect due to the density and distribution of source points or the distance threshold used to define dispersal capability.

Conclusions: This work provides one of the first comparisons of spatial predictions of different methods, frameworks, and parameterizations of connectivity models. Our results support environmental planning by clarifying what most influences predictions of movement patterns and how the predicted connectivity networks differ between different analytical frameworks.

1. Introduction

Connectivity between populations and habitats is important for a wide range of ecological processes (Cushman et al., 2016; Huang et al., 2020; Rudnick et al., 2012). In Europe, these issues have been the impetus of the Natura2000 program, which aims to create a series of

protected areas for the entire continent. To succeed in achieving a robust and effective connectivity network, it is necessary to use models and metrics that take into account numerous factors related to ecology and additional variables that make these indicators reliable (Kaszta et al., 2020a; Macdonald et al., 2013; Rudnick et al., 2012).

To understand, preserve, and restore landscape connectivity, several

* Corresponding author.

E-mail addresses: giovanni.lumia@unirc.it (G. Lumia), giuseppe.modica@unime.it (G. Modica), salvatore.pratico@unirc.it (S. Praticò), sam.cushman@gmail.com (S. Cushman).

<https://doi.org/10.1016/j.ecoinf.2024.102678>

Received 14 August 2023; Received in revised form 4 May 2024; Accepted 7 June 2024

Available online 13 June 2024

1574-9541/© 2024 The Author(s). Published by Elsevier B.V. This is an open access article under the CC BY license (<http://creativecommons.org/licenses/by/4.0/>).

methods have emerged to simulate movement and connectivity across the landscape. These different methods produce predictions of landscape connectivity (Foltête et al., 2012b; Cushman et al., 2016; Cushman & Lewis, 2010; Kevin McGarigal, 2000) from a functional perspective. All connectivity metrics, indices and modeling strategies we evaluate in this paper have in common the objective of predicting the patterns of movement of organisms through a landscape that has spatially heterogeneous patterns of resistance to organism movement. In our case, by the term “connectivity prediction” we mean the spatial predictions and maps produced by the different connectivity algorithms we compared in this paper. This entails building ecological networks based on natural areas that can sustain ecological functionality (Natura 2000 project, link: https://environment.ec.europa.eu/topics/nature-and-biodiversity/natura-2000_en; last access 31 January 2024), reflecting the hypothesized movement of organisms across gradients of landscape resistance. However, few studies have compared the results from these different strategies and how they are related to each other. Studies have compared how connectivity is affected by different patch sizes, number of nodes, and topological variables (De Montis et al., 2019). Other approaches have compared the properties of connectivity metrics calculated at the level of individual landscape elements (e.g., nodes or patches) and those at the global level (Niquil et al., 2020). Although these studies compared indices or connectivity metrics belonging to a specific model. This topic is important, as little is known about the relative differences of methods or the influences of dispersal threshold and spatial analysis framework on the predictions of connectivity modeling.

A study done by Cushman et al. (2013) showed that dispersal distance and the distribution of source points across the landscape influence connectivity predictions, where a synoptic point distribution gave more accurate results than a patch-based one. Additionally, several researchers have recently compared the performance of different connectivity methods (Cushman et al., 2014; Lumia et al., 2024; de Jonge et al., 2021; Unnithan Kumar and Cushman, 2022; Zeller et al., 2018). Cushman et al. (2014) found significant differences in spatial prediction between resistant kernel and factorial least cost path models and that for that analysis, the factorial least cost path had nominally better performance. However, the resistant kernel was more stable and generalizable. Zeller et al. (2018) found that cost distance approaches, like resistant kernels, were generally more robust and accurate than circuit theory approaches in explaining observed movement patterns. Most recently, Unnithan Kumar and Cushman (2022) simulated a large pool of dispersal processes and compared their congruence with the predictions of different connectivity models run on the same resistance surfaces and the same sets of source points. They found that resistant kernels were almost always the most accurate and robust predictor of functional connectivity, whereas factorial least-cost paths were always the worst. They found circuit theory predictors were occasionally the best when there was a strong destination bias in animal movement and when those destinations were known to the observer and included in the analysis. However, none of these or other comparative studies of connectivity methods have formally compared the similarities and differences of connectivity predictions concerning the combination of the analysis method, dispersal threshold used, and spatial framework (patch-centroid based vs. synoptic).LuL

In this study, we focus on how connectivity predictions were affected by three factors: different analysis methods, different dispersal thresholds, and different spatial frameworks for delineating source points or nodes for analysis. For the last of those topics, we have distinguished between patch centroid-based source points and spatially synoptic source points distributed across patches at a density proportional to habitat suitability.

We used different methods to calculate connectivity metrics to fill this knowledge gap. First, we used the Graphab software to obtain a network composed of patches and corridors. A node was assigned for each patch following graph theory (patch-based approach). Different

connectivity indices were calculated for each node. Subsequently, we used UNICOR to calculate and map a series of corridors based on the resistant kernels system (<https://github.com/ComputationalEcologyLab/UNICOR>.- last access 1 April 2024). In this system, nodes were not allocated to patches but generated probabilistically in a proportional suitability manner (synoptic approach).

Subsequently, several statistical analysis techniques were used to compare them. In particular, we proposed four main and several others combination hypotheses. We hypothesized that differences in the results of connectivity analyses might be mainly related to different dispersal thresholds (H1); synoptic vs. patch-based source points (H2); differences in methods, specifically kernel, path, and graph metrics (H3); and UNICOR connectivity value vs. several graph-theoretical metrics calculated in Graphab environment (H4); To evaluate these hypotheses, we employed Principal Component Analysis (PCA), hierarchical agglomerative clustering analysis (Kevin McGarigal, 2000), and Mantel testing on model matrices (which is a multivariate distance-based analysis of variance testing categorical hypotheses, e.g., Legendre, 1998). The main objective of this work was to evaluate the relationships among different approaches used for calculating landscape connectivity.

2. Materials and methods

The study area is located in southern Italy (Fig. 1) and includes the territory of 12 municipalities, accounting for nearly 50,000 ha. The area includes plains along the coastal strip, occupied mainly by meadows and cultivated with temporary or permanent crops. In the inland belt, we find hilly areas, from 100 to 600 m above sea level, occupied by permanent crops or shrubs typical of the Mediterranean maquis. In the northeastern part of the study area, we find the mountainous zone, which ranges from 600 to 1700 m above sea level and includes deciduous, coniferous, and shrub forests. This area includes part of the Aspromonte National Park.

The analysis presented here was structured in three steps: (1) collection and organization and processing (through free and open source software) of datasets of both cartographic aspects of the study area and the autecological characteristics of focal species (habitat, home range dispersal distance, affinity level to land cover); (2) construction of an ecological network and calculation of connectivity metrics; (3) comparison and statistical analysis of networks and connectivity metrics. At this stage, the two scenarios compared are the outputs of UNICOR and Graphab, two of the most important exponents of Kernel density (the former) and graph theory (the latter) connectivity methods.

The product of these elaborations was a set of maps that we defined as “surface of predicted connectivity”. Those are maps produced by the connectivity software (e.g. resistant kernel density and factorial least cost path density for UNICOR) patch assignment of Graphab connectivity metrics (from the centroid to all pixels in the patch). The correlation analysis were run out through the pixel values of each of these surfaces with each other surface to see how similar the spatial predictions of connectivity were between the methods.

2.1. Data collection and processing

Data referring to the land cover provided by the European Copernicus program, Corine Land Cover (CLC) 2018, and Urban Atlas (UA) 2018 were used to define landscape patterns for our analysis (Copernicus, Land Monitoring Service: <https://land.copernicus.eu/>-last access 17/02/2022). CLC has a minimum mappable unit of 25 ha (where 25 ha is the area of the smallest polygon of the vector land cover map) and 25 different land cover classes; it was made with the aim of representing the natural areas of Europe according to 5 hierarchical class levels. With 27 land cover classes, UA has a minimum mappable unit of 0.25 ha for class 1 areas (urban centers, factories, human-made areas, etc.) and 1 ha for the remaining categories from 2 to 5. UA was made to represent the major urban areas of Europe. It was therefore decided to integrate these

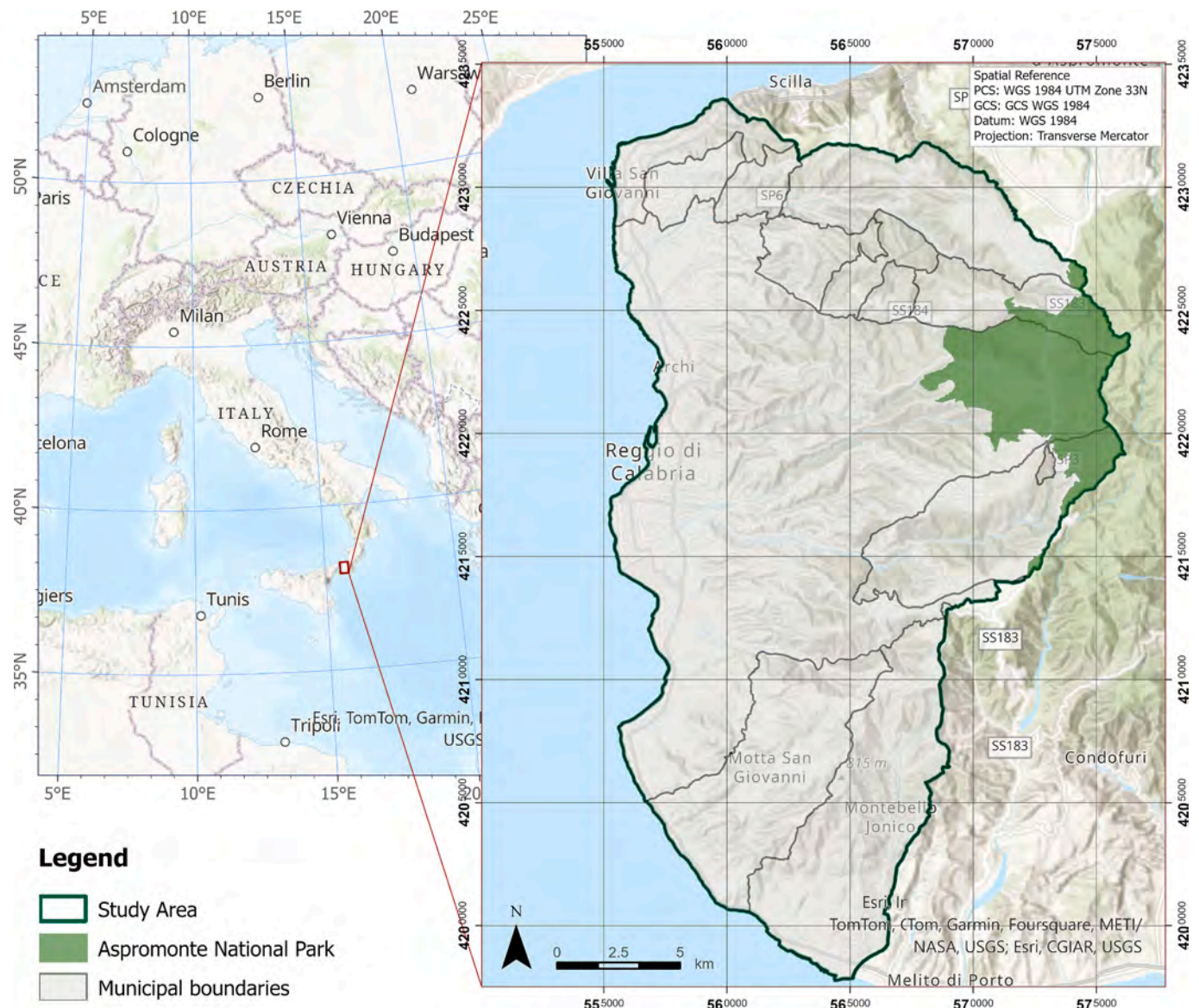


Fig. 1. Geolocalization of the study area, the metropolitan area of Reggio Calabria, in southern Italy. The map also shows the area falling within the Aspromonte National Park (in light green). (For interpretation of the references to colour in this figure legend, the reader is referred to the web version of this article.)

two data since CLC was designed to represent natural areas, so it completely omits highly artificial areas such as roads, highways, buildings, etc., elements that were instead represented with a high level of detail by the UA. Therefore, the final dataset was composed of class 1 from UA and classes 2–5 from CLC (Fig. 2).

Drawing on the work of Boitani et al. (2002), our analysis represents the collective central tendency of connectivity of 10 mammal species in terms of their habitat associations and movement abilities (see Appendix, Table A1). Considering that the goal of our work is not to create an ecological network but to test the differences between different approaches, we decided to identify this set of 10 species, which would serve solely as a model for the study area across life history space. We took the data from the 10 species to find a value in the middle, which gives a measure of the central tendency of connectivity. The decision to select only small and medium-sized mammals is related to their more significant proximity in terms of the amount of resources they need, perception of their surroundings, ability to overcome obstacles (vertical walls, buildings, roads), and the distances they need to cross. In order to make reliable predictions, we relied on data collected by Boitani et al. (2002) on the behavioral and autecological properties of the selected

species. This information gives values referring to each species' dispersal distance, home range, and affinity level with a given environment. The choice of the species was based on work already done in the same area (Lumia et al., 2023, 2024; Modica et al., 2021), and selection was made by giving priority to species protected by national and international laws (<https://www.mite.gov.it/pagina/repertorio-della-fauna-italiana-protetta> - last accessed 16/02/2022).

The integration of UA and CLC was performed in the QGIS 2.8 environment. The geometries coded as class 1 (artificial areas) of UA were merged into CLC. The minimum mappable unit of the obtained data was UA, being less than CLC. See Lumia et al. (2023) for more information about that process. The vector layer was converted to a raster with a spatial resolution of $2.5 \text{ m} \times 2.5 \text{ m}$ to allow subsequent processing. Then, through a bilinear interpolation operation, we resampled the pixel size up to $10 \text{ m} \times 10 \text{ m}$. The data thus obtained were used in the subsequent analyses below. After carefully inspecting the 2.5 m datum, we evaluated the possibility of used bilinear interpolation to increase the pixel size while retaining the fundamental information of the base map. The choice of 10 m was considered a fair compromise, allowing us to reduce the estimated calculation time.

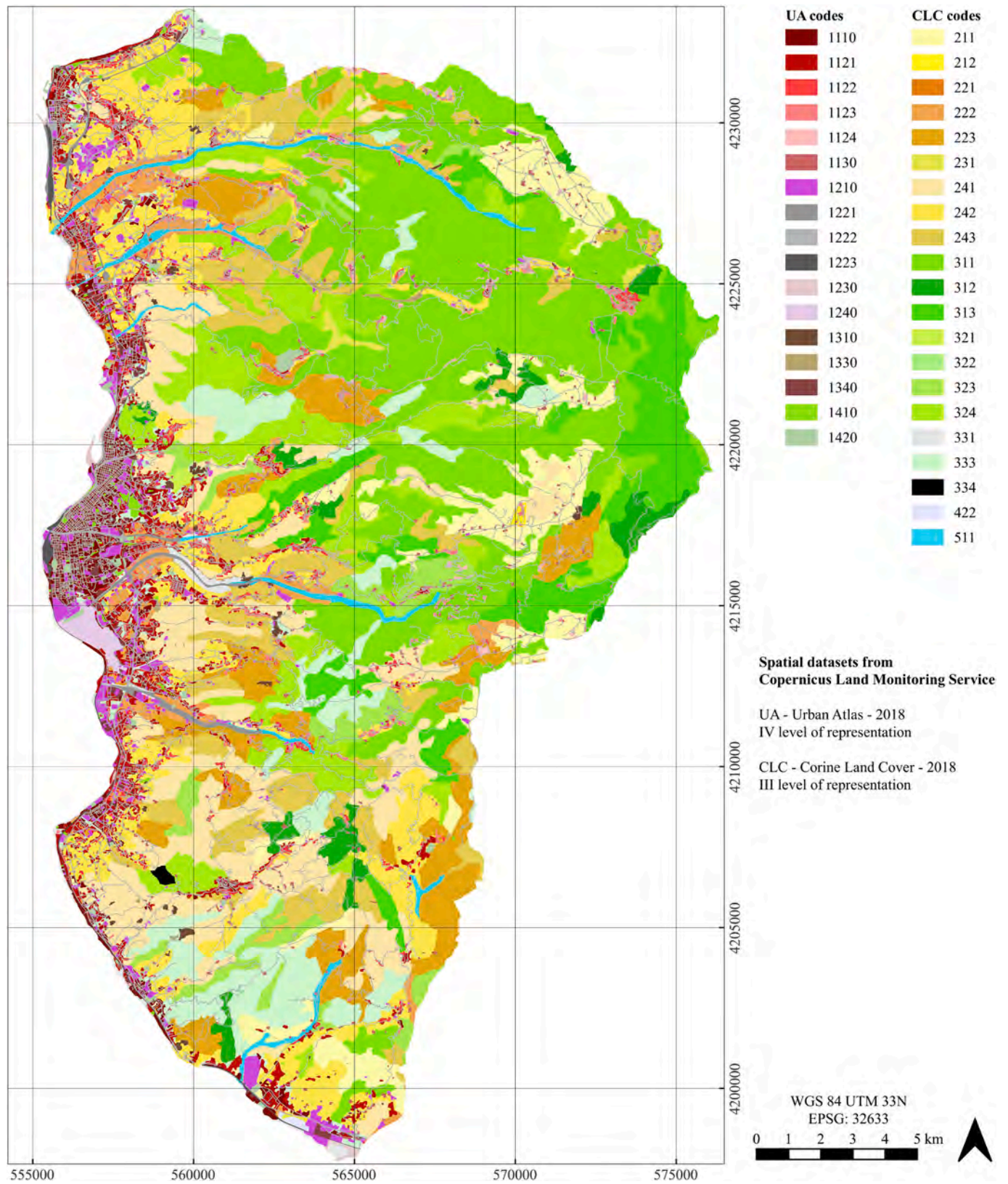


Fig. 2. Map of the implemented dataset using Corine Land Cover (CLC) 2018 for classes 2 (Agricultural areas), 3 (Forest and seminatural areas), 4 (Wetlands) and 5 (Water bodies), and Urban Atlas (UA) 2018 for class 1 (Artificial Surfaces).

2.2. Graphab implementation

Graphab 2.6 was used to construct the multi-species ecological network of the entire study area (Clauzel & Godet, 2020; Foltête et al., 2012a; Ersoy et al., 2019; Foltête et al., 2012a; Godet and Clauzel, 2021). It is compatible with GIS software, which makes it versatile and capable of providing significant support to those working in cartography and planning (Clauzel & Godet, 2020). This software was designed for

constructing and visualizing graphs, and it is capable of connectivity analysis and links to external data (<https://sourcesup.renater.fr/www/graphab/en/home.html> - last accessed 22/01/2023). Before launching operations in Graphab, we considered the characteristics of the 10 focal species. First, an affinity level between the species and each different land cover class was identified (Table 1). Different land cover types show different permeability depending on the mobility of the species passing through them (Cushman et al., 2012; Lechner and Lefroy, 2014).

Table 1

This table shows the characteristics of the 10 selected species, including land cover resistance values, dispersal ability, and home range. Land use codes from 11100 to 14200 refer to Urban Atlas 2018, whereas codes from 21000 to 51100 refer to Corine Land Cover 2018 (S.L. stands for surface land).

Urban Atlas + Corine Land Cover combined legend	<i>Martes foinea</i>	<i>Martes martes</i>	<i>Felis silvestris</i>	<i>Hystrix cristata</i>	<i>Sciurus Vulgaris</i>	<i>Eliomys quercinus</i>	<i>Erinaceus europaeus</i>	<i>Glis glis</i>	<i>Mustela nivalis</i>	<i>Muscardinus avellanarius</i>
Animal home range (ha)	10	140	124	20	2	2	2	2	8	2
Animal dispersal threshold (m)	5000	10,000	150,000	2000	2000	2000	2000	2000	3400	2000
Land use code	Resistance values [1 = no resistance, 100 = very high resistance]									
11100	Continuous urban fabric (S.L. > 80%)	100	100	100	100	100	100	100	100	100
11210	Discontinuous dense urban fabric (S.L. 50% - 80%)	100	100	100	100	100	100	100	100	100
11220	Discontinuous medium density urban Fabric (S.L. 30% - 50%)	100	100	100	100	100	100	100	100	100
11230	Discontinuous low-density urban fabric (S.L. 10% - 30%)	100	100	100	100	100	100	100	100	100
11240	Discontinuous very low-density urban fabric (S.L. < 10%)	100	100	100	100	100	100	100	100	100
11300	Isolated dtructures	100	100	100	100	100	50	50	100	100
12100	Industrial, commercial, public, military and private units	100	100	100	100	100	100	100	100	100
12210	Fast transit roads and associated lands	100	100	100	100	100	100	100	100	100
12220	Other roads and associated lands	50	50	100	70	100	100	100	70	100
12230	Railways and associated lands	100	100	100	100	100	100	100	100	100
12300	Port areas	100	100	100	100	100	100	100	100	100
12400	Airports	100	100	100	100	100	100	100	100	100
13100	Mineral extraction and dumpsites	100	100	100	100	100	100	100	100	100
13300	Construction sites	100	100	100	100	100	100	100	100	100
13400	Land without current use	50	50	50	50	50	50	50	50	50
14100	Green urban areas	50	50	50	50	50	50	50	50	50
14200	Sport and leisure facilities	100	100	100	100	100	100	100	100	100
21000	Arable land	25	25	50	25	50	25	50	25	50
21100	Non-irrigated arable land	25	25	50	25	50	25	50	25	50
21200	Permanently irrigated land	25	25	50	25	50	25	50	25	50
22100	Vineyards	75	75	75	75	75	75	75	75	75
22200	Fruit trees and berry plantations	50	50	50	50	50	50	50	50	50
22300	Olive groves	50	50	50	50	50	50	50	50	50
23100	Pastures	25	25	50	25	50	25	50	25	50
24100	Annual crops associated with permanent crops	25	25	50	25	50	25	50	25	50
24200	Complex cultivation patterns	75	75	75	75	75	75	75	75	75
24300*	Land principally occupied by agriculture, with significant areas of natural vegetation	1	1	1	1	1	1	1	1	1
31100*	Broad-leaved forest	1	1	1	1	1	1	1	1	1
31200*	Coniferous forest	1	1	1	1	1	1	1	1	1
31300*	Mixed forest	1	1	1	1	1	1	1	1	1
32000*	Scrub and/or herbaceous vegetation associations	1	1	1	1	1	1	1	1	1
32100*	Natural grasslands	25	25	50	25	50	25	50	25	50
32200*	Moors and heathlands	1	1	1	1	1	1	1	1	1
32300*	Sclerophyllous vegetation	1	1	1	1	1	1	1	1	1
32400*	Transitional woodland-shrub	1	1	1	1	1	1	1	1	1
33100	Beaches, dunes, sands	75	75	75	75	75	75	75	75	75
33300*	Sparsely vegetated areas	25	25	50	25	50	25	50	25	50
33400	Burnt areas	50	50	50	50	50	50	50	50	50
42200	Salines	100	100	100	100	100	100	100	100	100
51100	Water courses	1	1	1	1	1	1	1	1	1

* Land use codes considered for patches.

We then identified from these values the one in the middle that would meet the needs of a hypothetical (average) species living in the study area and used this to attribute the final resistance surface. A possible difficulty for some animals to swim was excluded in attributing resistance to watercourses. The reason for this is linked to the nature of Calabrian watercourses, which are dry or have such a low water flow that they can be crossed without the need to swim.

As explained in Lumia et al. (2023), a slope factor was also considered in constructing the network. In particular, areas with a slope >100% were excluded from being considered patches. In addition, the Graphab software allows through a function related to the following equation to consider slope when calculating corridors:

$$r_{\text{final}} = r^*(1 + c \cdot p) \quad (1)$$

In Eq. (1), p is the importance of the slope, c is the weighting coefficient, r is the pixel resistance, and r_{final} is the pixel resistance weighted by the slope (p). When $c = 1$, the resistance value is doubled for a slope of 10%, whereas if $c = 10$, the resistance is doubled for a slope of 100% ($p = 1$). Since in this work we considered the value of the coefficient c to be 1, as the slope increases, the permeability decreases.

The input data processed in Graphab consisted of a categorized raster land cover map. The nodes of the graph (patches) correspond to land cover classes that we defined as optimal for the selected species. Next, we defined a threshold of 2000 m as the maximum according to two types of distance, Euclidean and minimum cost. In our case, we used the minimum-cost system, starting from assigning resistance values to each land-cover category ranging from 1 (lowest impedance to movement) to 100 (barrier to movement). Subsequently, we identified 2000 m as the valid dispersal distance to meet each species' minimum requirements (Boitani et al., 2002, see also Table 1). Next, we defined a threshold of 2000 m as the maximum distance that each species can travel (Boitani et al., 2003; Jones et al., 2018).

The simulation allows the animal to cross 2000 pixels having resistance 1 before stopping. The software makes the animal move in such a way that starting from the first pixel, it always chooses the adjacent pixel with minimum cost. Its movement stops when the sum of the resistances of the crossed pixels equals the value of 2000 cost units. A species' maximum affinity (land cover with resistance = 1) to a particular land cover had been considered a possible habitat. The home range, defined here as the extent of land large enough to contain the resources necessary to complete the individual's life cycle (Boitani et al., 2003), was used to set a threshold of 2 ha for the inclusion of patches as nodes for the patch-based analyses since this value is suitable for all the selected species (Table S1). That threshold was used for the inclusion of patches as nodes for the patch-based analyses. Only areas with a surface area greater than or equal to 2 ha were considered nodes in the graph network; remaining areas with an area <2 ha were only considered structural elements favorable to the passage of species.

To identify the dispersal distance, a crossing threshold was established for all focal species, understood as the maximum distance an animal can travel in a hostile environment to reach resources. The values were taken from literature (Boitani et al., 2003).

Starting from the 10 m × 10 m raster containing the land cover codes and minimum patch size, land cover resistance, and maximum dispersal threshold, Graphab 2.6 was launched. It returns a series of nodes and arcs that are the graphic representation of patches and ecological corridors, respectively (Foltête et al., 2012b). We set up the software so that all the arcs between patches are potentially taken into account, even those that might intersect or partially overlap. This method was used as it does not exclude any possible pathways and provides an initial linear representation of displacements, allowing for a realistic representation of ecological corridors (Godet and Clauzel, 2021).

Graphab was then used to calculate a number of graph-theoretical metrics at the node level. These indices characterize the network, quantifying its connectivity and identifying its elements of centrality

(Foltête et al., 2012a; Bodin & Saura, 2010; Pascual-Hortal and Saura, 2006; Saura and Pascual-Hortal, 2007; Urban and Keitt, 2001). This was done by calculating the following metrics (See appendix A2): Integral Index of Connectivity (IIC), Betweenness Centrality (BC), Flux (F) and Probability of Connectivity (PC).

2.3. UNICOR implementation

Before launching UNICOR, following the same process used for Graphab, each pixel of the base map raster was assigned a resistance value to movement in a range from 1 (low resistance) to 100 (high resistance), with resistance values tending toward unity, indicating land cover with higher species affinity, lower resistance to species movement; values tending toward 100 indicate anthropogenically modified land-cover types, lower species affinity and higher resistance to movement.

UNICOR requires two input datasets for model implementation: a raster layer representing the landscape resistance surface and a txt file containing the coordinates of source points of individuals. One of the major strengths of UNICOR connectivity modeling is the ability to specify biologically realistic dispersal thresholds, specified in cost units, at which the connectivity algorithms (factorial least cost path and resistant kernel) terminate their spread. It is essential for connectivity analyses to realistically reflect the functional dispersal capabilities of focal species, given that this, along with the density and distribution of source points, often dominates predictions of functional connectivity (e.g., Cushman et al., 2012). In our analyses, we evaluated a range of plausible biological capabilities (Diniz et al., 2020; Lechner et al., 2015; Savary et al., 2021).

Our UNICOR analyses considered both patch-based and synoptic frameworks. Patch-based approach refers to a situation where an amount of node is selected a priori, considering a certain number of spots as the only places where the animal movement is considered likely to occur. "Synoptic" refers to an approach in which connectivity is measured among a large number of source points that are distributed proportional to the extensiveness of highly suitable and low resistance habitat (e.g., many points in areas of low resistance instead of a single point in the centroid of a patch of low resistance). The patch-based framework used the 320 centroids of patches used as nodes in the Graphab analysis. The number of 320 comes from the number of total patches obtained by applying our criteria: land cover with a maximum affinity for species (Table 1); minimum area of polygons to be considered patches of 2 ha; slope lower than 100%. We ran factorial least cost path and resistant kernel analyses for these source points at three dispersal distances in meters: 50 k, 100 k and 150 k. For the synoptic approach, we used a network of 3243 source points that were probabilistically generated with density proportional to habitat suitability and used dispersal distances of 17 k and 35 k for resistant kernel and factorial least cost path, respectively, reflecting the expected cost distance to traverse 2 km in geographic space (17 k) or twice that for factorial least cost path analysis (it is expected to use a larger threshold for factorial least cost path analysis, as it is pairwise and requires twice the distance threshold for points to be linked by paths as points to be overlapping in resistant kernel analysis; e.g., Cushman et al., 2013, 2014). The value of 3243 was obtained by random assignment of a series of points but with a higher probability directly proportional to the suitability of the study area (inverted resistance values). The approach we used to obtain the points is based on a series of processes. We created a raster with the same extension as the land cover raster but with random pixel values between 0 and 0.75. Next, the resistance values we had attributed to land cover were converted to suitability and then rescaled, going from 1 to 100 to 0–1. Finally, we overlaid the two layers (the one with values from 0 to 0.75 and the one with values from 0 to 1) and calculated the difference. Finally, one point was assigned for each pixel with a value >0.

The values of 50 k, 100 k, 150 k, 17 k, and 35 k were taken to be applied to the two different approaches, synoptic and patch-based. In UNICOR, the simulation allows the movement simulation to be

calculated based on an energy budget. Thus, there is a relationship between the residual energy of the animal (the hypothetical animal moving in the software simulation) and the number of steps remaining. However, the ability of the animal to move varies with the heterogeneity of the pixel matrix (land cover raster). Therefore, it is possible to obtain the total energy value of the animal from the formula $\text{step} \times \text{cost}$. This is directly related to dispersal capacity, the expected dispersal distance in steps (mean cost of resistance surface \times the number of steps in the path) = energy budget, or number of steps = energy budget / mean cost of resistance surface. So, given the mean resistance value of the matrix, which is 85, the value of 2 km (the value we had identified in the literature as being reachable by all the considered species) is equivalent to an energy budget of 17 k. This is due to the mean resistance of 85 and pixel size of 10. Then, a 2 km distance will equal 85 average cost units per pixel \times 200 pixels in 2 km = 17 k cost units for 2 km. We used this value twice for the factorial least cost path, resulting in the 35 k value. This is because it had been proved that twice the dispersal distance is needed to connect two points by factorial least cost path to have kernels overlapping in resistant kernel analysis (Cushman et al., 2013).

2.4. PCA, hierarchical agglomerative clustering and mantel testing of hypotheses

The analyses described above produced 12 scenarios of predicted connectivity for comparison (Table 2). These included a patch-based approach for factorial least cost path and resistant kernel connectivity, using 50 k, 100 k and 150 k dispersal thresholds (p50k, p100k, p150k, k50, k100 and k150, respectively); the connectivity metrics BC, F, PC and IIC produced on these same source point nodes; and synoptic analyses using source points synoptically distributed across the study area proportionally to habitat suitability to seed factorial least cost path 35 k (sp35k) and resistant kernel 17 k (sk17).

We proposed 4 main hypotheses of relationship among the 12 different scenarios. These were: (1) thresh – that methods using a similar dispersal distance threshold would be more similar in their predicted connectivity than methods using different thresholds, (2) synoptic – that scenarios using a synoptic framework would be more similar to each other than to scenarios that used a patch-based framework, (3) kernel-path-graph – that kernel methods would be more similar to each other in predicted connectivity than to path methods or graph methods and the converse, (4) UNICOR-graph – that connectivity methods using UNICOR approaches would produce connectivity results more similar to each other than to graph metrics and the converse. The relationships

Table 2
Description of the 12 connectivity scenarios compared in this analysis.

Scenario acronym	Scenario description
p50k	Patch-centroid-based factorial least cost path with 50,000 cost unit threshold
p100k	Patch-centroid-based factorial least cost path with 100,000 cost unit threshold
p150k	Patch-centroid-based factorial least cost path with 150,000 cost unit threshold
k50k	Patch-centroid based factorial resistant kernel with 50,000 cost unit threshold
k100k	Patch-centroid based factorial resistant kernel with 100,000 cost unit threshold
k150k	Patch-centroid based factorial resistant kernel with 150,000 cost unit threshold
sp35k	Synoptic factorial least cost path with 35,000 cost unit threshold
sp17k	Synoptic factorial least cost path with 17,000 cost unit threshold
IIC	Patch-centroid-based graph theory metric Integral Index of Connectivity
PC	Patch-centroid-based graph theory metric Probability of Connectivity
F	Patch-centroid-based graph theory metric Flux
BC	Patch-centroid-based graph theory metric Betweenness Centrality

between the different items are expressed in the form of correlation. What has been done is to compare the different scenarios and to see whether the values of one approach go up, so does the other, or vice versa.

We used Mantel testing with model matrices (Legendre, 1998), which is a form of multivariate, distance-based analysis of variance. We tested the four main hypotheses and the additive combination of the various model matrices to test for joint support of multiple hypotheses simultaneously (e.g., Kyaw et al., 2021). Thus, we used the Mantel test to identify the correlation between the 4 hypotheses and 14 different combinations of them (Table 3).

In addition to the hypothesis testing with Mantel model matrix analysis, we used two well-known multivariate analysis methods to compare the 12 scenarios. Specifically, we used Principal Component Analysis (PCA) and hierarchical agglomerative clustering analysis on the 12 scenarios and visually compared the results in reference to the Mantel hypothesis testing. The PCA was conducted on the correlation matrix and the hierarchical clustering was conducted using Ward's fusion distance method in the 'hclust' function in R.

3. Results

3.1. principal component analysis

The principal component analysis revealed that variance among the connectivity scenarios was relatively well concentrated on a few independent orthogonal dimensions (Table 3). Specifically, the first PC captured about 38% of the variance among connectivity predictions and 63.5% by the first two.

The correlation matrix (Table 4) shows that the highest correlations were between the different dispersal distance thresholds among kernel and path analyses, with higher values of correlation found for correlations between p100k-p150k (0.99) and k100k-k150k (0.99). The next highest correlations were found between the patch-based path and the patch-based kernel (e.g., path with path and kernel with kernel) with values ranging from 0.92 to 0.99. The synoptic path is relatively highly correlated with the patch-based path (0.71, 0.65, 0.62). Likewise, the synoptic kernel is relatively highly correlated with the patch-based kernel (0.77, 0.59, 0.55). The metric IIC is not highly correlated with any path or kernel analyses (most correlated with the synoptic kernel, 0.28). The metric PC is not highly correlated with any of the kernel or path values except the synoptic kernel (0.41). The metric F is highly correlated with the synoptic kernel (0.62). The metric BC is also correlated with the synoptic kernel (0.45).

The biplot (Fig. 3 and supplementary materials) of the PCA analysis shows three things: (1) most importantly, the graph-theoretical metrics were all highly related to the resistant kernel metrics (in Fig. 3, the vectors in blue were relatively parallel for these), (2) the factorial least cost path metrics were all quite different from the kernel and the graph-theoretical metrics (blue vectors for those were almost perpendicular toward the top from the kernel and graph-theoretical metrics), (3) the synoptic models (sk17 and sp34; e.g., UNICOR with many sources points proportional to suitability across the landscape instead of the centroid of the patches) were highly correlated with the patch-centric approach (e.g., highly parallel to the vectors).

3.2. Hierarchical agglomerative clustering

The hierarchical clustering (Fig. 4) shows the same general relationships as the PCA in a slightly different way. Specifically, the hierarchical clustering shows that: (1) the path analyses were all clustered separately (to the left of the diagram), (2) the kernel analyses were clustered together to the right, with the metric F most similar to the synoptic kernel. The other graph-theoretical metrics were clustered (IIC, PC, BC) and relatively similar to the kernel analyses.

Table 3

Values of standard deviation, proportion of variance and cumulative proportion for the 12 scenarios (PC1, ...PC12).

Importance of components	PC1	PC2	PC3	PC4	PC5	PC6
Standard deviation	21,235	17,633	11,445	101,538	0,83,504	0.69050
Proportion of Variance	0.3758	0.2591	0.1092	0.08592	0.05811	0.03973
Cumulative Proportion	0.3758	0.6349	0.7440	0.82995	0.88806	0.92779
//	PC7	PC8	PC9	PC10	PC11	PC12
Standard deviation	0.66373	0.54153	0.28398	0.21220	0.06356	0.05454
Proportion of Variance	0.03671	0.02444	0.00672	0.00375	0.00034	0.00025
Cumulative Proportion	0.96450	0.98894	0.99566	0.99942	0.99975	1.00000

Table 4

Correlation matrix of the 12 different scenarios. Gray indicates the diagonal. In red values >0.9, yellow 0.9 > x > 0.8, dark green 0.8 > x > 0.7 and light green 0.7 > x > 0.6.

	p50k	p100k	p150k	k50k	k100k	k150k	sp35k	sk17k	IIC	PC	F	BC
p50k	1	0.96	0.92	0.22	0.21	0.2	0.71	0.15	0.09	0.05	0.15	0.06
p100k	-	1	0.99	0.08	0.08	0.08	0.65	0.07	0.06	0.01	0.11	0.03
p150k	-	-	1	0.03	0.02	0.03	0.62	0.05	0.04	0	0.09	0.02
k50k	-	-	-	1	0.93	0.88	0.26	0.77	0.24	0.34	0.48	0.29
k100k	-	-	-	-	1	0.99	0.21	0.59	0.2	0.29	0.37	0.23
k150k	-	-	-	-	-	1	0.2	0.55	0.19	0.27	0.35	0.21
sp35k	-	-	-	-	-	-	1	0.28	0.12	0.11	0.22	0.13
sk17k	-	-	-	-	-	-	-	1	0.28	0.41	0.62	0.45
IIC	-	-	-	-	-	-	-	-	1	0.52	0.19	0.13
PC	-	-	-	-	-	-	-	-	-	1	0.23	0.21
F	-	-	-	-	-	-	-	-	-	-	1	0.29
BC	-	-	-	-	-	-	-	-	-	-	-	1

3.3. Mantel testing of hypotheses

Based on a significance level of 0.05 (*p*-value), 12 of the 14 hypotheses were supported. In Table 5, we order these hypotheses based on the strength of their Mantel *r* value. Hypothesis 3, which tests for differences among kernel, path and graph theory methods, combining other factors (dispersal distance, patch-based vs. synoptic), had the strongest correlation value with an *r* of -0.711. The next highest support was for H6, which is a combination of kernel_path_graph and dispersal threshold effects. The fact that this combined hypothesis is less supported (*r*-value ~0.18 lower in magnitude) suggests that adding the effect of dispersal threshold to the effect of the analysis method reduces the ability to explain the differences in the connectivity results. Likewise, the next set of most-supported hypotheses combines the method (kernel_path_graph) with other factors such as synoptic or the combination of synoptic and threshold. The reduced support of these combined hypotheses suggests that the method is the dominant driver of differences in predictions and threshold and that synoptic vs. patch-based source points had a relatively small influence. The least support of all hypotheses was for H2, synoptic vs patch-based source points. Furthermore, the 4 hypotheses with the lowest support in addition to H2 were composite hypotheses containing H2, suggesting that synoptic vs. patch-based analysis had the least influence on the difference in connectivity results.

4. Discussion

The PCA, clustering, and correlation analyses all generally supported the same conclusions. Namely, least cost path methods were different in their predictions and clustered and ordinated separately from other methods. Surprisingly, kernel and graph-theoretical metrics were generally closely aligned, notably the synoptic kernel with the Flux parameter (F). Notably, dispersal threshold and synoptic vs. patch-based parameters did not appear to strongly separate results, which were highly aligned with the analysis method. This suggests that overall patterns of the connectivity prediction were relatively insensitive to changes in dispersal ability, at least across the range (50,000 to 150,000

cost units) evaluated in this study. Similarly, the multivariate results and correlation analysis show minimal relative effect of using patch-centric source points vs synoptic source points. The results suggest that resistant kernel predictions were highly consistent with the graph-theoretical metrics but were superior in that the resistant kernel produces predictions synoptically (for all locations) rather than just the centroid of the cells (Cushman et al., 2013; Unnithan Kumar and Cushman, 2022). The kernel analysis based on the centroids is similar to the synoptic kernel. However, the synoptic kernel is better since it considers biologically realistic dispersal ability and the correct distribution and density of source points (Cushman et al., 2013).

Analyzing the results of Mantel testing of hypotheses, we found that the highest support was for H3, suggesting that the largest difference among connectivity predictions is related to the method of analysis, with kernel, path, and graph theory approaches being different from each other.

The second most supported hypothesis was the H6, where we combined the kernel_path_graph hypothesis (H3) and the dispersal threshold hypothesis. The dispersal threshold hypothesis proposes that the dispersal distance used in the analysis is the main factor affecting the difference in results, whereas methods (kernel, path, graph theory) and framework (patch-based vs. synoptic) were not influential. The combination of these two hypotheses asks if the method (kernel, path, graph theory) and dispersal distance were both important. Observing substantially lower support for this joint hypothesis than for H3 confirms that the method of analysis is the dominant driver of differences and that the dispersal threshold is relatively less impactful.

The third most highly supported hypothesis was H10, where we combined H3 and H4. This gives relatively more similarity weight to UNICOR methods compared to graph theory methods but still discriminates between kernel and least cost path approaches. The lower Mantel *r* value for this hypothesis compared to H3 suggests that the dominant difference is between kernel, path and graph theory metrics and that adding additional similarity weight for path and kernel vs graph theory metrics did not improve the explanation of the differences in predictions.

The fourth most supported hypothesis was H13, similar to the third, except adding the additional factor of synoptic vs. patch-based source points. This resulted in a substantial decrease in the Mantel *r* value, suggesting adding the effect of synoptic vs. patch-based source points to the model matrix decreased the ability to explain differences in prediction. This, along with the observation that the pure synoptic vs patch-based hypothesis (H2) is the least supported of all hypotheses and is not statistically related to differences in connectivity predictions, suggests that synoptic vs. patch-based methods were relatively similar compared to the differences in results caused by other factors, particularly method (H3). Similarly, the fourth most supported hypothesis was the same as the first (H3), except including the additive model matrix effects of synoptic vs patch-based and dispersal threshold. The observation that this hypothesis was substantially less supported than the pure method hypothesis (H3) suggests that adding the influences of dispersal threshold and synoptic vs. patch-based analysis decreases the ability to statistically explain the differences among connectivity predictions. Considering the 7 most supported hypotheses were those in which H3 is present alone or in combination with other hypotheses, we had further

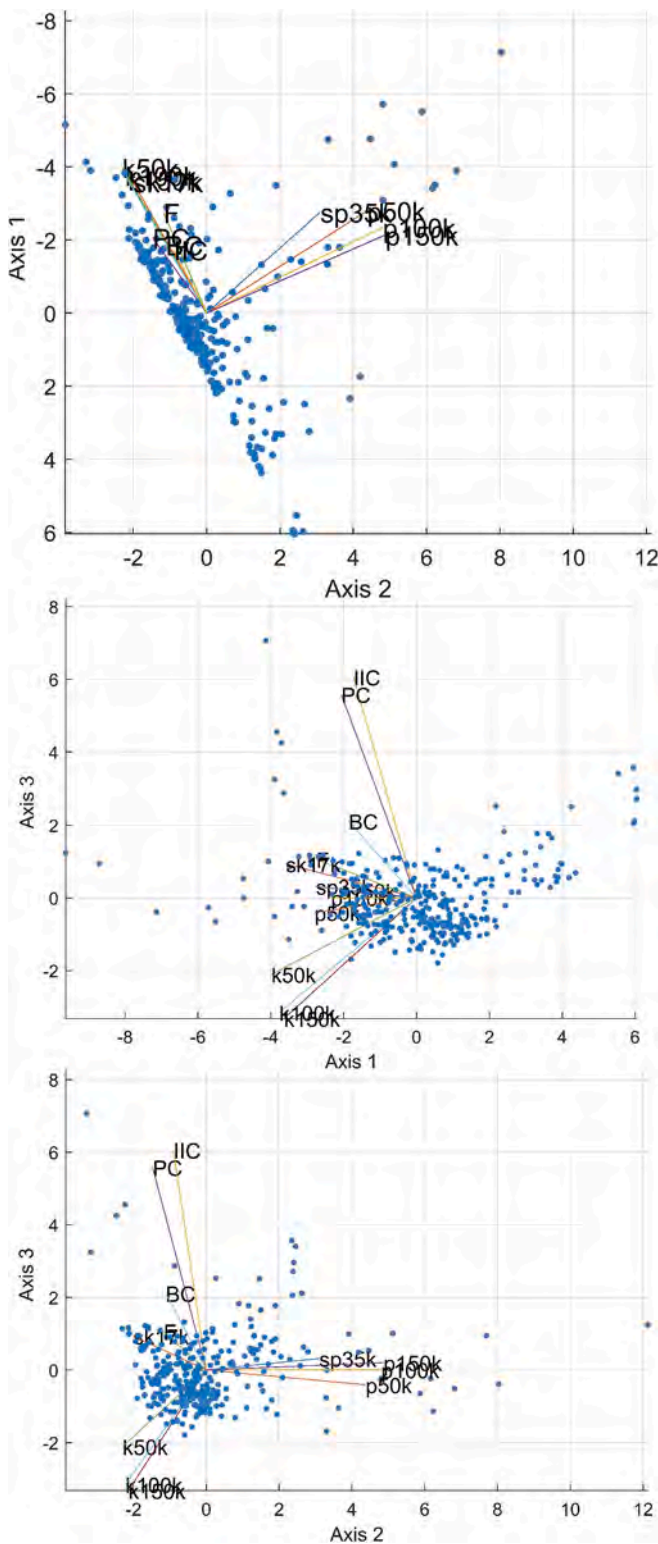


Fig. 3. Biplot of the PCA analysis, a) Axis 1 vs Axis 2, b) Axis 1 vs Axis 3, c) Axis 2 vs Axis 3.

confirmation that differences among connectivity results were dominated by the analysis method.

All four testing methods (correlation matrix, PCA, hierarchical clustering, model matrix, Mantel hypothesis testing) corroborate the same major interpretation. The analysis method (in our case, least cost path, resistant kernel, and graph theory metrics) dominates differences in connectivity predictions. The least cost path methods produce a tight

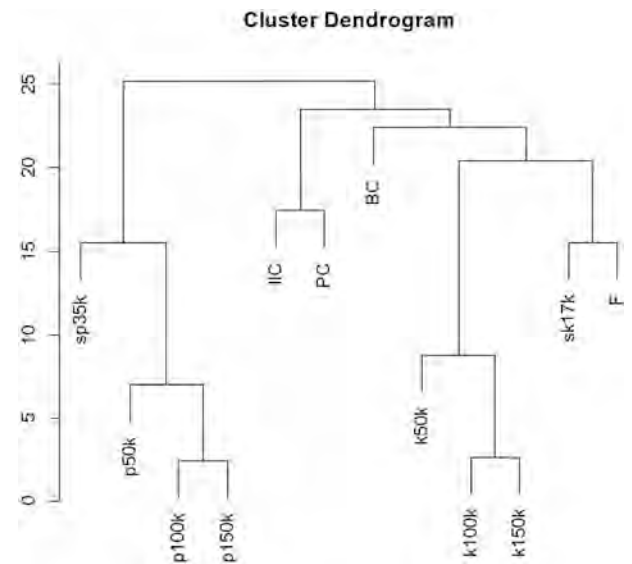


Fig. 4. Clustering dendrogram of the 12 scenarios.

cluster or cloud in ordination space and differ in prediction from the other methods. Conversely, resistant kernel and graph theory metrics were generally highly congruent, notably the synoptic kernel and the Flux parameter (F) from graph theory.

Importantly, our results clearly show that the dispersal threshold and density and distribution of source points had much less relative influence than the analysis method. This is very interesting, given that other studies, e.g., Cushman et al. (2012), found large differences in predictions produced by a given method (e.g., resistant kernels) based on dispersal threshold and density and distribution of source points. The discrepancy in these results is likely because this previous study compared results for a particular method (such as least cost path or resistant kernel) while varying dispersal threshold and source point density and distribution. These previous papers showed substantial effects of dispersal ability and source point density but did not formally compare the relative effects of different methods. Our study is novel in combining evaluation of all these factors as main effects and in interaction. Our novel finding is that analysis methods, in particular, least cost path, kernel and graph theory approaches, produce dramatically different predictions whose divergence dwarfs the effects caused by differences in dispersal threshold or the density and distribution of source points.

Given the predominant effect of the method and the observation that kernel and graph theory methods group together in clustering and ordination space, our results suggest that resistant kernel might be the preferred approach among those we evaluated. We conclude this partly based on the recent study by Unnithan Kumar and Cushman (2022), who showed, using a large simulation factorial experiment, that resistant kernel predictions had the highest similarity to movement patterns for a wide range of hypothetical organisms following a broad combination of movement rules. The similarity of the kernel and graph theory methods suggests that both approaches were likely robust. However, the resistant kernel is preferred in most cases as the graph theory approach generally produces predictions only for a smaller sample of nodes or centroids of patches. In contrast, the resistant kernel approach produces a fully synoptic prediction of movement density (incidence function, (Kasza et al., 2020b)) across the full landscape. This provides a rich, spatially explicit mapping of movement patterns and density, which allows the delineation of core areas, identification of barriers and prioritization of corridors (Cushman et al., 2016, 2018; Cushman and Landguth, 2012; Kasza et al., 2018, 2021; Macdonald et al., 2019).

Table 5
14 different correlation hypotheses.

Hypotheses n°			r	P
h3	kernel_path_graph	3	-0.71196	0.001
h6	thresh_kernel_path_graph	13	-0.57854	0.001
h10	kernel_path_graph_unicor_graph	34	-0.57773	0.002
h13	synoptic_kernel_path_graph_unicor_graph	234	-0.45688	0.005
h11	thresh_synoptic_kernel_path_graph	123	-0.43879	0.003
h14	thresh_synoptic_kernel_path_graph_synoptic_unicor_graph	1234	-0.43182	0.007
h8	synoptic_kernel_path_graph	23	-0.40205	0.002
h4	unicor_graph	4	-0.34138	0.006
h7	thresh_unicor_graph	14	-0.33068	0.019
h1	Thresh	1	-0.31747	0.021
h12	thresh_synoptic_unicor_graph	124	-0.24275	0.033
h9	synoptic_unicor_graph	24	-0.16499	0.082
h5	threst_synoptic	12	-0.11937	0.162
h2	Synoptic	2	0.141494	0.18

5. Conclusions

In this paper, we studied the relationships between several different methods, parameterizations, and metrics by which assessments of landscape connectivity were commonly made in the literature. In particular, we studied how connectivity predictions were influenced by different analysis methods, dispersal thresholds, and spatial frameworks for delineating source points. We clarified that what most influences predictions is the method of analysis. Specifically, we found that resistant kernel-based analysis is the most suitable for representing movement patterns. This study provided expanded knowledge regarding differences and similarities in the predictions of commonly used approaches in landscape connectivity by demonstrating through statistical analyses (PCA, clustering, Mantel test of hypotheses) how strong relationships exist between some of them and major differences between others. While highlighting which variables most influence connectivity predictions, our analysis did not indicate the best methods for predicting functional connectivity to delineate corridors or the ideal network configuration. In those cases, species-related factors such as energy (Movement simulation where the animal moves randomly until it runs out of energy), attraction (Movement simulation where the animal moves non-randomly and follows the path of least resistance) and risk (Movement simulation where the animal had an increasing probability of stopping its movement by crossing more and more pixels with resistance values) should be taken into account to identify what is the best configuration of the method (Lumia et al., 2024), dispersal threshold and spatial framework so as to be able to provide a tool to the intervention planner. Future research should explore the functional performance of these and other connectivity methods in predicting functional connectivity.

Appendix A. Appendix

Table A1
National and international legislation protecting the identified focal species.

Species	L. 157/92 art. 2 (1)	L. 157/92 (2)	BERNA Ap.2 (3)	BERNA Ap.3 (4)	CITES All. A (5)	CITES All. B (6)	HABITAT Ap.4 (7)	HABITAT Ap.5 (8)	IUCN (9)
<i>Martes foina</i>		x		x					
<i>Martes martes</i>	x			x				x	
<i>Felis silvestris</i> Schreber	x		x			x			
<i>Hystric cristata</i>		x	x				x		x
<i>Sciurus vulgaris</i> L.		x			x				x
<i>Eliomys quercinus</i>		x		x					x

(continued on next page)

Author contributions

All authors contributed to the general co-production of this work, revised it and agreed on its content.

Funding

This work was not supported by specific funding.

CRediT authorship contribution statement

Giovanni Lumia: Writing – review & editing, Writing – original draft, Visualization, Validation, Software, Resources, Methodology, Investigation, Formal analysis, Data curation, Conceptualization. **Giuseppe Modica:** Writing – review & editing, Visualization, Validation, Supervision, Resources, Project administration, Methodology, Investigation, Funding acquisition, Formal analysis, Data curation, Conceptualization. **Salvatore Praticò:** Writing – review & editing, Resources, Investigation, Formal analysis. **Samuel Cushman:** Writing – review & editing, Validation, Supervision, Resources, Methodology, Investigation, Formal analysis, Data curation, Conceptualization.

Declaration of competing interest

The authors declare that they have no known competing financial interests or personal relationships that could have appeared to influence the work reported in this paper.

Data availability

Data will be made available on request.

Table A1 (continued)

Species	L. 157/92 art. 2 (1)	L. 157/92 (2)	BERNA Ap.2 (3)	BERNA Ap.3 (4)	CITES All. A (5)	CITES All. B (6)	HABITAT Ap.4 (7)	HABITAT Ap.5 (8)	IUCN (9)
<i>Erinaceus europaeus</i> L.		x		x					x
<i>Glis glis</i>		x		x					
<i>Mustela nivalis</i> L.		x		x					
<i>Muscardinus avellanarius</i>		x		x			x		x

- (1) Standards for the protection of homeothermic wildlife and hunting harvest, species specifically protected in Article 2 of the Law of February 11, 1992. Convention on the Conservation of Migratory Species of Wild Animals.
- (2) Standards for the protection of homeothermic wildlife and hunting, species protected by the law of February 11, 1992. Convention on the Conservation of Migratory Species of Wild Animals.
- (3) Annex 2 of the Convention on the Conservation of European Wildlife Habitats, adopted in Bern on September 19, 1979.
- (4) Annex 3 of the Convention on the Conservation of European Wildlife Habitats, adopted in Bern on September 19, 1979.
- (5) Regulation on protecting wild fauna and flora species by regulating trade therein. Species listed in Annex A of Regulation (EC) No. 2307/97.
- (6) Regulation on protecting wild fauna and flora species by regulating trade therein. Species listed in Annex B of Regulation (EC) No. 2307/97.
- (7) Annex 4 to Habitats Directive 43/92/EEC called Animal and Plant Species of Community Interest Requiring Strict Protection. Updated with Council Directive 97/62/EC of October 27, 1997.
- (8) Annex 5 to Directive 43/92/EEC “Habitats” named Animal and plant species of Community interest whose taking in the wild and exploitation could be subject to management measures. Updated with Council Directive 97/62/EC of October 27, 1997.
- (9) Belonging to one of the categories assigned by the International Union for Conservation of Nature (IUCN), which identify the conservation status of animal and plant species by assigning categories listed on the so-called Red List: extinct; extinct in the wild; critically endangered; endangered; vulnerable; lower risk; protection dependent; near risk; relative risk; insufficient data; not assessed.

Table A2

Ecological, graph theory connectivity indices calculated in the present work.

Connectivity index	Ecological meaning	Formula	Reference
Integral Index of Connectivity (IIC)	The probability that individuals randomly located in the landscape within a patch can access each other. A higher value indicates a higher connectivity.	$\frac{\sum_{i=1}^n \sum_{j=1}^n a_i^* a_j}{1 + n l_{ij}}$	Freeman, (1977)
Betweenness Centrality (BC)	The sum of the shortest paths through the focal patch, each path being weighted by the product of the connected patches’ capacities and their interaction probability.	$BC_i = \sum_k \sum_j a_i^k a_k^j e^{-ad_{jk}}$ $j, k \in \{1..n\}, k < j,$ $i \in P_{jk}$	(Bodin and Saura, 2010)
Flux (F)	For the entire graph: sum of the potential dispersions of all patches.	$F = \sum_{i=1}^n \sum_{j=1, j \neq i}^n a_i^j e^{-ad_{ij}}$	(Foltête et al., 2012b)
Probability of Connectivity (PC)	The probability that two random points in the landscape fall within interconnected habitat areas (i.e., reachable to each other). Values are between 0 and 1.	$PC = \frac{\sum_{i=1}^n a_i a_j p_{ij}^*}{A_L^2}$	(Saura and Pascual-Hortal, 2007)

Appendix B. Supplementary data

Supplementary data to this article can be found online at <https://doi.org/10.1016/j.ecoinf.2024.102678>.

References

Bodin, Orjan, Saura, Santiago, 2010. Ranking individual habitat patches as connectivity providers: integrating network analysis and patch removal experiments. *Ecol. Model.* 221 (19), 2393–2405. <https://doi.org/10.1016/J.ECOLMODEL.2010.06.017>.

Boitani, L., Corsi, F., Faluccci, A., Marzetti, I., Masi, M., Montemaggiore, A., Ottaviani, D., Reggiani, G., Rondinini, C., 2002. Rete Ecologica Nazionale. Un approccio alla conservazione dei vertebrati italiani. In: Università di Roma “La Sapienza”, Dipartimento di Biologia Animale e dell’Uomo; Ministero dell’Ambiente, Direzione per la Conservazione della Natura; Istituto di Ecologia Applicata.

Boitani, L., Faluccci, A., Maiorano, L., Montemaggiore, A., 2003. Italian Ecological Network: the Role of Protected Areas in the Conservation of Vertebrates (I. of A. E. Animal and Human Biology Department, University of Rome “La Sapienza”, Nature Conservation Directorate of the Italian Ministry of Environment, Ed.).

Clauzel, C., Godet, C., 2020. Combining spatial modeling tools and biological data for improved multispecies assessment in restoration areas. *Biological Conservation* 250, 108713. <https://doi.org/10.1016/j.biocon.2020.108713>.

Cushman, S.A., Landguth, E.L., 2012. Multi-taxa population connectivity in the Northern Rocky Mountains. *Ecol. Model.* 231, 101–112. <https://doi.org/10.1016/j.ecolmodel.2012.02.011>.

Cushman, S.A., Landguth, E.L., Flather, C.H., 2012. Evaluating the sufficiency of protected lands for maintaining wildlife population connectivity in the U.S. northern Rocky Mountains. *Divers. Distrib.* 18 (9), 873–884. <https://doi.org/10.1111/j.1472-4642.2012.00895.x>.

Cushman, S.A., Landguth, E.L., Flather, C.H., 2013. Evaluating population connectivity for species of conservation concern in the American Great Plains. *Biodivers. Conserv.* 22 (11), 2583–2605. <https://doi.org/10.1007/s10531-013-0541-1>.

Cushman, S., Lewis, J., Landguth, E., 2014. Why did the bear cross the road? Comparing the performance of multiple resistance surfaces and connectivity modeling methods. *Diversity* 6 (4), 844–854. <https://doi.org/10.3390/d6040844>.

Cushman, S.A., Elliot, N.B., Macdonald, D.W., Loveridge, A.J., 2016. A multi-scale assessment of population connectivity in African lions (*Panthera leo*) in response to landscape change. *Landscape Ecol.* 31 (6), 1337–1353. <https://doi.org/10.1007/s10980-015-0292-3>.

Cushman, S.A., Elliot, N.B., Bauer, D., Kesch, K., Bahaa-el-din, L., Bothwell, H., Flyman, M., Mtare, G., Macdonald, D.W., Loveridge, A.J., 2018. Prioritizing core

- areas, corridors and conflict hotspots for lion conservation in southern Africa. *PLoS One* 13 (7). <https://doi.org/10.1371/journal.pone.0196213>.
- Cushman, S.A., Lewis, J.S., 2010. Movement behavior explains genetic differentiation in American black bears. *Landscape Ecology* 25 (10), 1613–1625. <https://doi.org/10.1007/s10980-010-9534-6>.
- de Jonge, V.N., Schückel, U., 2021. A comprehensible short list of ecological network analysis indices to boost real ecosystem-based management and policy making. *Ocean & Coastal Management* 208, 105582. <https://doi.org/10.1016/j.ocecoaman.2021.105582>.
- De Montis, A., Ganciu, A., Cabras, M., Bardi, A., Mulas, M., 2019. Comparative ecological network analysis: An application to Italy. *Land Use Policy* 81, 714–724. <https://doi.org/10.1016/j.landusepol.2018.11.043>.
- Diniz, M.F., Cushman, S.A., Machado, R.B., De Marco Júnior, P., 2020. Landscape connectivity modeling from the perspective of animal dispersal. *Landscape Ecol.* 35 (1), 41–58. <https://doi.org/10.1007/s10980-019-00935-3>.
- Ersoy, E., Jorgensen, A., Warren, P.H., 2019. Identifying multispecies connectivity corridors and the spatial pattern of the landscape. *Urban Forestry & Urban Greening* 40, 308–322. <https://doi.org/10.1016/j.ufug.2018.08.001>.
- Foltête, J.-C., Clauzel, C., Vuidel, G., 2012a. A software tool dedicated to the modelling of landscape networks. *Environ. Model Softw.* 38, 316–327. <https://doi.org/10.1016/j.envsoft.2012.07.002>.
- Foltête, J.-C., Clauzel, C., Vuidel, G., Gilles, Tournant, Pierline, 2012b. Integrating graph-based connectivity metrics into species distribution models. *Landscape Ecol.* 27 (4), 557–569.
- Freeman, L.C., 1977. A Set of Measures of Centrality Based on Betweenness. *Sociometry* 40 (1), 35. <https://doi.org/10.2307/3033543>.
- Godet, C., Clauzel, C., 2021. Comparison of landscape graph modelling methods for analysing pond network connectivity. *Landscape Ecol.* 36 (3), 735–748. <https://doi.org/10.1007/s10980-020-01164-9>.
- Huang, J., Andreollo, M., Martensen, A.C., Saura, S., Liu, D., He, J., Fortin, M., 2020. Importance of spatio-temporal connectivity to maintain species experiencing range shifts. *Ecography* 43 (4), 591–603. <https://doi.org/10.1111/ecog.04716>.
- Jones, K.R., Venter, O., Fuller, R.A., Allan, J.R., Maxwell, S.L., Negret, P.J., Watson, J.E.M., 2018. One-third of global protected land is under intense human pressure. *Science (New York, N.Y.)* 360 (6390), 788–791. <https://doi.org/10.1126/SCIENCE.AAP9565>.
- Kaszta, Z., Cushman, S.A., Sillero-Zubiri, C., Wolff, E., Marino, J., 2018. Where buffalo and cattle meet: modelling interspecific contact risk using cumulative resistant kernels. *Ecography* 41 (10), 1616–1626. <https://doi.org/10.1111/ecog.03039>.
- Kaszta, Z., Cushman, S.A., Macdonald, D.W., 2020a. Prioritizing habitat core areas and corridors for a large carnivore across its range. *Anim. Conserv.* 23 (5), 607–616. <https://doi.org/10.1111/acv.12575>.
- Kaszta, Z., Cushman, S.A., Macdonald, D.W., 2020b. Prioritizing habitat core areas and corridors for a large carnivore across its range. *Anim. Conserv.* 23 (5), 607–616. <https://doi.org/10.1111/acv.12575>.
- Kaszta, Z., Cushman, S.A., Slotow, R., 2021. Temporal non-stationarity of path-selection movement models and connectivity: an example of African elephants in Kruger National Park. *Front. Ecol. Evol.* 9 <https://doi.org/10.3389/fevo.2021.553263>.
- Kevin McGarigal, S.A.C.S.S., 2000. *Multivariate Statistics for Wildlife and Ecology Research*. Springer-Verlag New York, Inc.
- Kyaw, P.P., Macdonald, D.W., Penjor, U., Htun, S., Naing, H., Burnham, D., Kaszta, Z., Cushman, S.A., 2021. Investigating carnivore guild structure: Spatial and temporal relationships amongst threatened felids in myanmar. *ISPRS International Journal of Geo-Information* 10 (12), 808. <https://doi.org/10.3390/IJGI10120808/S1>.
- Lechner, A.M., Lefroy, E.C., 2014. *General Approach to Planning Connectivity from Local Scales to Regional (GAP CLoSr): Combining Multi-Criteria Analysis and Connectivity Science to Enhance Conservation Outcomes at Regional Scale (Issue March)*.
- Lechner, A.M., Doerr, V., Harris, R.M.B., Doerr, E., Lefroy, E.C., 2015. A framework for incorporating fine-scale dispersal behaviour into biodiversity conservation planning. *Landscape Urban Plan.* 141, 11–23. <https://doi.org/10.1016/j.landurbplan.2015.04.008>.
- Legendre, P., Legendre, Louis, 1998. *Numerical ecology*, 20. Elsevier Science & Technology, p. 853, 2012 Elsevier B.V.
- Lumia, G., Praticò, S., Di Fazio, S., Cushman, S., Modica, G., 2023. Combined use of urban atlas and Corine land cover datasets for the implementation of an ecological network using graph theory within a multi-species approach. *Ecol. Indic.* 148, 110150 <https://doi.org/10.1016/j.ecolind.2023.110150>.
- Lumia, G., Modica, G., Cushman, S., 2024. Using simulation modeling to demonstrate the performance of graph theory metrics and connectivity algorithms. *J. Environ. Manag.* 352, 120073 <https://doi.org/10.1016/j.jenvman.2024.120073>.
- Macdonald, D.W., Willis, K.J., Cushman, S.A., McRae, B., Adriaenssen, F., Beier, P., Shirley, M., Zeller, K., 2013. *Biological Corridors and Connectivity Chapter 21*.
- Macdonald, D.W., Bothwell, H.M., Kaszta, Z., Ash, E., Bolongon, G., Burnham, D., Can, Ö. E., Campos-Arceiz, A., Channa, P., Clements, G.R., Hearn, A.J., Hedges, L., Htun, S., Kamler, J.F., Kawanishi, K., Macdonald, E.A., Mohamad, S.W., Moore, J., Naing, H., Cushman, S.A., 2019. Multi-scale habitat modelling identifies spatial conservation priorities for mainland clouded leopards (*Neofelis nebulosa*). *Divers. Distrib.* 25 (10), 1639–1654. <https://doi.org/10.1111/ddi.12967>.
- Modica, G., Praticò, S., Laudari, L., Ledda, A., Di Fazio, S., De Montis, A., 2021. Implementation of multispecies ecological networks at the regional scale: analysis and multi-temporal assessment. *J. Environ. Manag.* 289, 112494 <https://doi.org/10.1016/j.jenvman.2021.112494>.
- Niquil, N., Haraldsson, M., Sime-Ngando, T., Huneman, P., Borrett, S.R., 2020. Shifting levels of ecological network's analysis reveals different system properties. *Philosophical Transactions of the Royal Society B* 375 (1796). <https://doi.org/10.1098/RSTB.2019.0326>.
- Pascual-Hortal, L., Saura, S., 2006. Comparison and development of new graph-based landscape connectivity indices: towards the prioritization of habitat patches and corridors for conservation. *Landscape Ecol.* 21 (7), 959–967. <https://doi.org/10.1007/s10980-006-0013-z>.
- Rudnick, D.A., Ryan, S.J., Beier, P., Cushman, S.A., Dieffenbach, F., Epps, C.W., Gerber, L.R., Hartter, J., Jenness, J.S., Kintsch, J., Merenlender, A.M., Perkl, R.M., Preziosi, D.V., Trombulak Stephen, C., Rudnick, D., Rudnick, A., 2012. The role of landscape connectivity in planning and implementing conservation and restoration priorities. *Ecol. Soc. Am.* 16 (16), 1–23.
- Saura, S., Pascual-Hortal, L., 2007. A new habitat availability index to integrate connectivity in landscape conservation planning: comparison with existing indices and application to a case study. *Landscape Urban Plan.* 83 (2–3), 91–103. <https://doi.org/10.1016/j.landurbplan.2007.03.005>.
- Savary, P., Foltête, J., Moal, H., Vuidel, G., Garnier, S., 2021. Analysing landscape effects on dispersal networks and gene flow with genetic graphs. *Mol. Ecol. Resour.* 21 (4), 1167–1185. <https://doi.org/10.1111/1755-0998.13333>.
- Unnithan Kumar, S., Cushman, S.A., 2022. Connectivity modelling in conservation science: a comparative evaluation. *Sci. Rep.* 12 (1), 16680. <https://doi.org/10.1038/s41598-022-20370-w>.
- Urban, J.D., Keitt, T., 2001. *Landscape connectivity: a graph-theoretic perspective*. Wiley Behav. Ecol. Soc. Am. Stable 82 (5), 1205–1218.
- Zeller, K.A., Jennings, M.K., Vickers, T.W., Ernest, H.B., Cushman, S.A., Boyce, W.M., 2018. Are all data types and connectivity models created equal? Validating common connectivity approaches with dispersal data. *Divers. Distrib.* 24 (7), 868–879. <https://doi.org/10.1111/ddi.12742>.